Journal of Materials Science and Chemical Engineering, 2025, 13(8), 28-46
https://www.scirp.org/journal/msce
ISSN Online: 2327-6053
ISSN Print: 2327-6045

Electrochemical Oxidation of Methylene Blue by Cyclic Voltammetry on a Boron-Doped Diamond Electrode in Various Supporting Electrolytes

Evelyne Marie Hélène Loba, Foffié Thiery Auguste Appia, Kouadio Fulgence Yao, Tiémélé Ghislaine Désirée Kouassi, Lassiné Ouattara*, Kwa-Koffi Edith Kouassi*

Laboratoire de Constitution et Réaction de la Matière, UFR SSMT, Université Félix Houphouët-Boigny, Abidjan, Côte d'Ivoire
Email: *ouatlassine@yahoo.fr, *edithkouassi77@yahoo.fr

How to cite this paper: Loba, E.M.H., Appia, F.T.A., Yao, K.F., Kouassi, T.G.D., Ouattara, L. and Kouassi, K.-K.E. (2025) Electrochemical Oxidation of Methylene Blue by Cyclic Voltammetry on a Boron-Doped Diamond Electrode in Various Supporting Electrolytes. *Journal of Materials Science and Chemical Engineering*, **13**, 28-46.
https://doi.org/10.4236/msce.2025.138003

Received: June 20, 2025
Accepted: August 12, 2025
Published: August 15, 2025

Abstract

In this study, the electrochemical behavior of methylene blue (MB) dye was investigated at a boron-doped diamond (BDD) electrode in various supporting electrolyte solutions. The physical characterization of the BDD surface by scanning electron microscopy (SEM) reveals a polycrystalline structure with grain sizes ranging between 0.3 and 0.6 µm. With Raman spectroscopy, the BDD surface is composed of diamond-type carbon (Csp3) and graphitic-type carbon (Csp2). Electrochemical characterization of the BDD electrode in 0.1 M H_2SO_4 and Na_2SO_4 solutions showed the presence of an anodic wave close to the onset potential of oxygen evolution. In the presence of MB, four anodic peaks and one cathodic peak were recorded in both media. Analysis of the first anodic and cathodic peaks suggests a quasi-reversible electrochemical process. In 0.1 M NaOH, the electrochemical response revealed a distinct anodic peak associated with oxygen evolution. The oxidation of MB in this basic medium was characterized by a broad anodic wave beginning within the potential window for water stability on the BDD electrode. The results obtained across the different electrolytes indicate that methylene blue can be oxidized either through direct electron transfer at the electrode surface or indirectly via reactive oxidative species generated in solution. The electrochemical process is diffusion-controlled, and in all three media, the formation of a polymeric film on the electrode surface was observed. These findings confirm the suitability of BDD electrodes for the electrochemical investigation and quantification of methylene blue.

Keywords

Electrochemical Oxidation, Cyclic Voltammetry, BDD, Methylene Blue Dye

1. Introduction

Dyes are organic compounds widely used in various sectors, including the paper, leather, cosmetics, food, printing, and especially the textile industries [1] [2]. Their intensive use meets a growing and increasingly diverse global demand, driven by the rapid increase in population. However, the presence of these compounds in the environment, even at low concentrations, represents a significant source of pollution. This contamination poses a threat to aquatic ecosystems and to human health [3]-[5].

Methylene blue (MB) is a heterocyclic aromatic dye of cationic nature, belonging to the thiazine family. It is widely used in various industrial sectors, particularly in textiles, biology, analytical chemistry, and medicine, due to its chemical stability and remarkable coloring properties [6]. However, this dye is recognized as a potentially hazardous compound for human health. Indeed, exposure to it can cause various adverse effects in humans, such as skin irritation, irreversible eye damage, nausea, vomiting, abdominal pain, headaches, increased blood pressure, and digestive disorders such as diarrhea [6]-[8]. Given these risks and the persistence of MB in the environment, it has become imperative to develop effective technologies for the removal of this organic pollutant from wastewater. To date, several processes have been explored for the treatment of MB, including adsorption, photolysis, photocatalysis, and anodic oxidation [9]-[13]. Regarding the electrochemical method, preparative electrolysis has proven to be highly effective for its degradation, especially when so-called non-active electrodes, such as the boron-doped diamond (BDD) electrode, are used at the anode [13]. This technology includes several techniques, among which cyclic voltammetry is commonly used.

Cyclic voltammetry is a fundamental electrochemical technique that provides valuable qualitative and quantitative information, particularly regarding the kinetic regime, anodic transfer coefficient, activation energy of electroactive species, and the nature of the involved reaction mechanisms. This technique also allows for the determination of the number of electrons exchanged during oxidation or reduction reactions, the theoretical potential of redox couples, the stoichiometry of the studied systems, the heterogeneous electron transfer rate constants, as well as the diffusion coefficients of species in solution. Owing to its sensitivity and versatility, cyclic voltammetry has been widely used to study the electrochemical behavior of various organic compounds such as pharmaceutical molecules [14], pesticides [15], and dyes [16]. Concerning organic compounds, Gnamba *et al.* studied the oxidation of amoxicillin, a model pharmaceutical compound, in a sulfuric acid (H_2SO_4) electrolyte solution using a boron-doped diamond (BDD) electrode as

the working electrode. The results showed that the oxidation of amoxicillin is a diffusion-controlled process. Moreover, this oxidation occurs via direct electron transfer at the electrode surface within the water stability window. Additionally, the sp^2 carbon located at the grain boundaries of the BDD electrode may contribute to the oxidation process at potentials close to the oxygen evolution reaction. Also, the study of successive cycles revealed the formation of a polymeric film on the electrode surface [14]. Similarly, the work conducted by Sun *et al.* on Alizarin Red S in sulfuric acid (H_2SO_4) using a boron-doped diamond (BDD) electrode revealed a diffusion-controlled oxidation process [17]. Furthermore, the formation of a polymeric film on the electrode surface was observed. Likewise, Tang *et al.* demonstrated that the oxidation of the X-6G dye on BDD in the presence of Na_2SO_4 also follows a diffusion-controlled mechanism [18].

However, most studies on the voltammetry oxidation of dyes in general, and methylene blue in particular are often limited to a single supporting electrolyte. In this context, we propose to investigate the electrochemical behavior of methylene blue in several supporting electrolytes (H_2SO_4, Na_2SO_4 and NaOH) using cyclic voltammetry. In this study, particular attention will be paid to the effects of compound concentration, scan rate, and successive voltammetry cycles. Additionally, the boron-doped diamond (BDD) working electrode employed in this study will be characterized using scanning electron microscopy (SEM) and Raman spectroscopy. To the best of our knowledge, no study has yet reported on the electrochemical behavior of methylene blue using the boron-doped diamond electrode as a working electrode in the three aforementioned aqueous media. We hope that this study will provide fundamental data that will be useful for future environmental and analytical applications.

2. Material and Methods

2.1. Reagents and Chemicals

Methylene blue (Chemical formula: $C_{16}H_{18}ClN_3S$; Purity > 98.0) was obtained from Aladdin Chemicals Co. Ltd. (Shanghai, China). Sulfuric acid (H_2SO_4) and sodium sulfate were produced by Merck. Sodium chloride (NaCl) and sodium hydroxide (NaOH) were manufactured by Merck. Stock solutions were prepared with distilled water. All experiments were carried out at laboratory temperature. All the chemicals used in this work were of analytical grade.

2.2. Measurement Procedure

Methylene blue solutions were prepared in different supporting electrolytes by dissolving the desired amount of MB in distilled water. Voltammograms were then recorded using an Autolab PGSTAT 20 connected to a computer.

2.3. Physical Characterization of the Boron-Doped Diamond (BDD) Electrode

The working electrode is a boron-doped diamond electrode with an active surface

area of 1 cm^2. This electrode was prepared by hot filament chemical vapor deposition (HF-CVD) on low-resistivity p-type silicon wafers (1 – 3 mΩ·cm) (Siltronix, 10 cm diameter, 0.5 mm thickness). The process gas was a mixture of 1% CH_4 in H_2 containing trimethylborane. The film growth rate was 0.24 $\mu m \cdot h^{-1}$. The film thickness was approximately 1 μm. Further details concerning the preparation of BDD electrodes are available in references [19] [20]. Scanning electron microscopy (SEM) images of the BDD electrode were taken using a JEOL LJMS-6300-F instrument.

2.4. Instrumentation and Analytical Procedure

The experimental setup consists of a three-electrode electrochemical cell composed of a working electrode (BDD) (working area was 1 cm^2), a counter electrode (Pt wire), and a reference electrode (saturated calomel electrode, SCE). These electrodes, immersed in a 100 mL solution, are connected to an Autolab potentiostat (ECHOCHEMIE PGSTAT 20) controlled by a computer (GPES software) allowing computerized data acquisition (**Figure 1**). The working electrode is fixed in a cage, facilitating contact between it and the electrolyte through an opening. The reference electrode is placed in a luggin capillary, the tip of which is positioned approximately 2 mm from the working electrode to minimize ohmic drop.

Before any voltammetric measurements, the electrodes are pretreated in a 0.1 M sulfuric acid solution by performing several cyclic voltammetry cycles at a scan rate of 50 mV/s during 10 minutes, with the goal of ensuring reproducibility and reliability of the results.

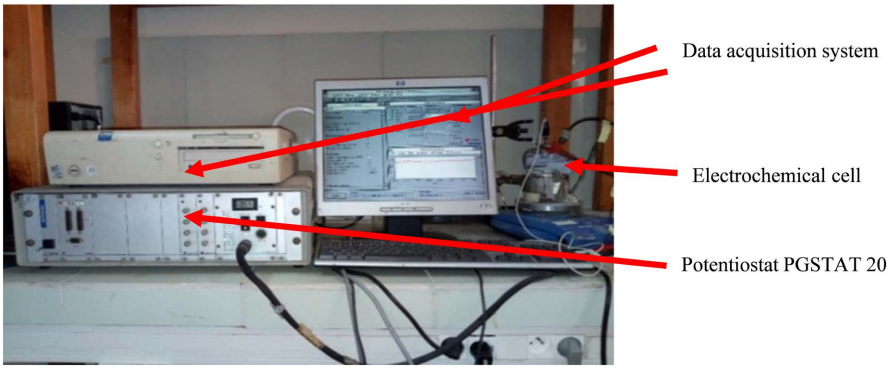

Figure 1. Experimental setup for electrochemical studies using a PGSTAT 20 potentiostat.

3. Results and Discussions

3.1. Physical Characterization of the BDD Electrode

The surface morphology of the boron-doped diamond electrode is shown in **Figure 2**. Scanning Electron Microscopy (SEM) reveals that the BDD has a polycrystalline structure [21]. The grain size ranges from 0.3 to 0.6 μm, and the grains are tightly bonded to each other. Additionally, a dark area is observed at the base of the diamond grains, particularly at the grain boundaries, likely related to graphitic carbon (Csp^2) formed during the preparation of the BDD.

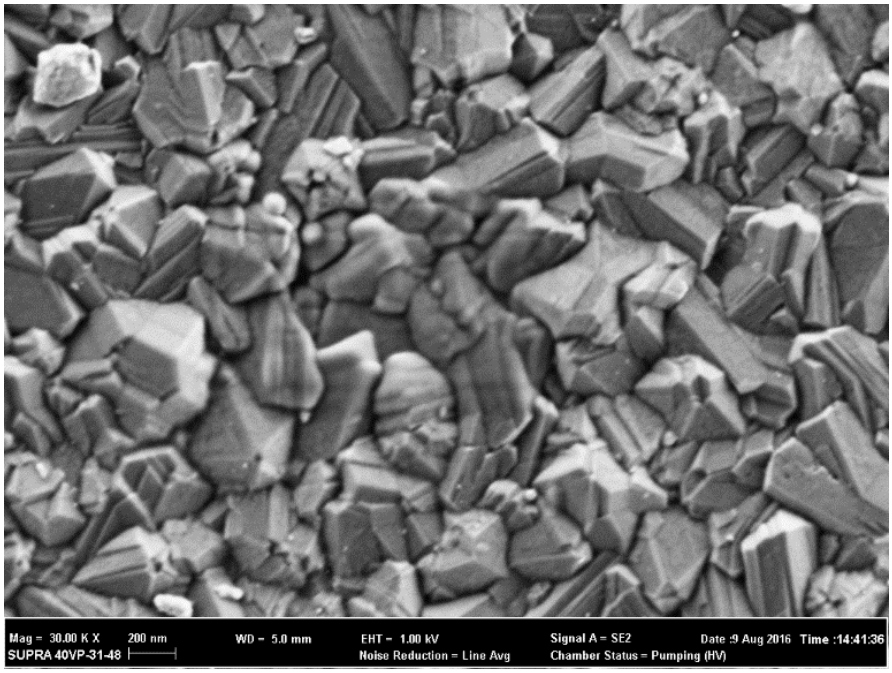

Figure 2. Surface appearance of the BDD electrode by SEM.

Figure 3 shows the Raman spectrum of the boron-doped diamond (BDD) sample, obtained under laser excitation at a wavelength of 514.5 nm. This spectrum reveals two intense peaks located at 500 cm^{-1} and 1332 cm^{-1}, attributed to silicon and diamond-type carbon (Csp^3), respectively. In addition, a broad band centered around 1550 cm^{-1}, characteristic of non-diamond carbon impurities (Csp^2), is also observed [22], which is consistent with the observation made using scanning electron microscopy (SEM). This observation suggests that graphitic carbon is present on the boron-doped diamond electrode, likely located at the grain boundaries of the diamond.

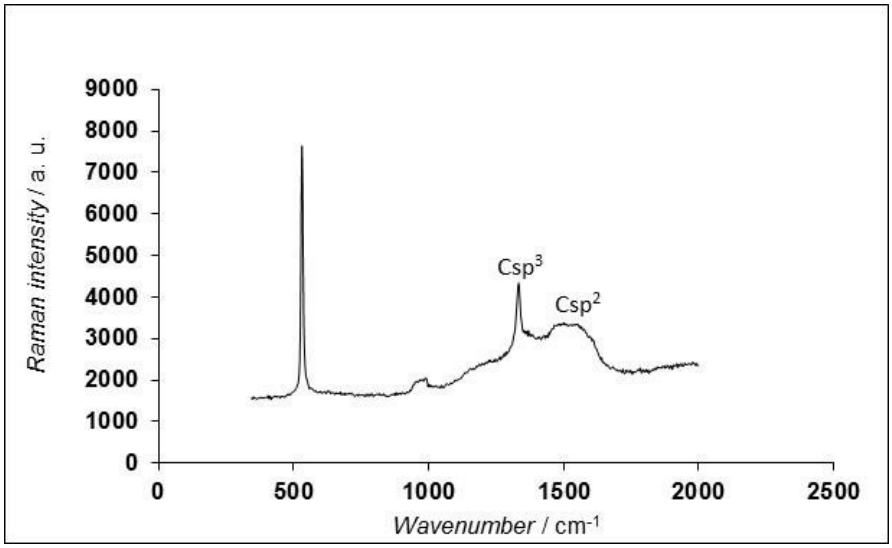

Figure 3. Raman spectroscopy spectrum of a BDD electrode.

3.2. Study of Oxidation in 0.1 M H_2SO_4 Medium

Figure 4 shows the cyclic voltammogram of the BDD electrode in 0.1 M H_2SO_4 medium in the absence of organic compound at 50 mV/s. The onset potentials for hydrogen and oxygen evolution can be clearly distinguished at −1.38 V and 1.84 V vs. SCE, respectively. Between the onset potentials of hydrogen and oxygen evolution, there is the electrochemical window of water stability at BDD electrode stability region, as well as an anodic wave between 1.40 and 1.85 V (highlighted in Figure 3). This wave could likely indicates the formation of oxidative sulfate species such as $SO_4^{\bullet-}$ and $S_2O_8^{2-}$ [23]-[25] in the supporting electrolyte. Species formation is described by equations (1) through (7). The formation of hydroxyl radicals results from the electrochemical decomposition of water on the BDD electrode (Equation 8). According to the literature, a sulfuric acid solution simultaneously contains sulfate ions, hydrogen sulfate anions, and undissociated sulfuric acid. However, only the latter two species react with hydroxyl radicals to generate sulfate radicals, as shown in equations (6) and (7) [25]. Moreover, according to Gnamba *et al.*, this anodic wave may be attributed to the oxidation of surface redox species such as Csp^2 especially surface quinone functional group [14].

$$SO_4^{2-} \rightarrow SO_4^{\bullet-} + e^- \quad (1)$$

$$HSO_4^- \rightarrow SO_4^{\bullet-} + H^+ + e^- \quad (2)$$

$$SO_4^{\bullet-} + HSO_4^- \rightarrow S_2O_8^{2-} + H^+ + e^- \quad (3)$$

$$SO_4^{2-} + SO_4^{\bullet-} \rightarrow S_2O_8^{2-} + e^- \quad (4)$$

$$SO_4^{\bullet-} + SO_4^{\bullet-} \rightarrow S_2O_8^{2-} \quad (5)$$

$$HSO_4^- + {}^{\bullet}OH \rightarrow SO_4^{\bullet-} + H_2O \quad (6)$$

$$H_2SO_4 + {}^{\bullet}OH \rightarrow SO_4^{\bullet-} + H_3O \quad (7)$$

$$H_2O \rightarrow {}^{\bullet}OH + H^+ + e^- \quad (8)$$

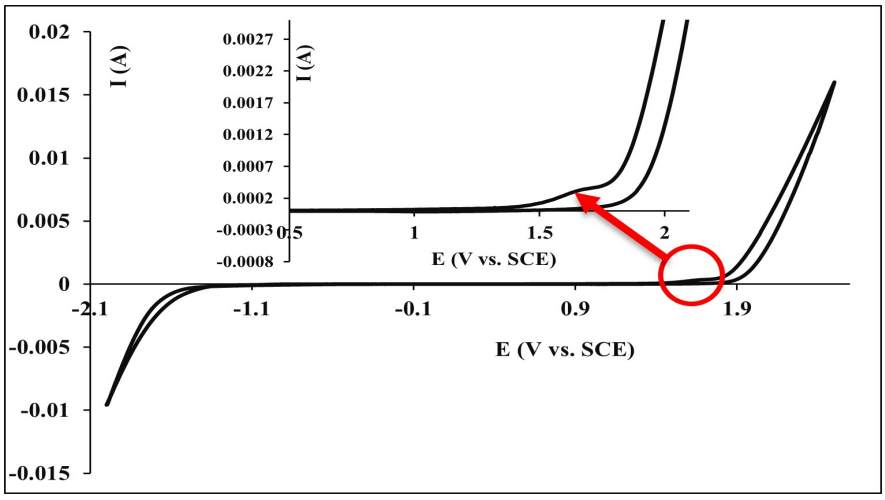

Figure 4. Cyclic voltammogram of the BDD in 0.1 M H_2SO_4 at 50 mV/s within the potential range of −2 to 2.6 V. WE: BDD, RE: SCE, and CE: Pt wire. Inset: Voltammogram of the BDD between 0.5 and 2 V.

Figure 5(A) shows the behavior of the boron-doped diamond electrode in the absence and presence of methylene blue (0.4 mM). This figure reveals that the oxidation of MB is characterized by four (04) anodic peaks and one cathodic peak located at 0.035, 0.94, 1.34, 1.57, and −0.063 V, respectively. All of these peaks appear before the oxygen evolution potential (1.84 V). However, Peak 4 appears within the potential domain associated with the formation of oxidative sulfate species, which may contribute to the oxidation of MB. These observations suggest that the oxidation of MB may occur via direct electron transfer and/or via oxidative species electro-generated in the reaction medium. The MB oxidation could also be catalyzed the non-diamond carbon impurities such as Csp2 presents at the BDD's grain boundaries [14]. Peaks 1 and 1' are attributed to the redox peaks of MB [26] [27].

In the following sections of this work, the investigations will focus exclusively on these two peaks. The difference between the anodic potential (Epa = 0.0497 V) and the cathodic potential (Epc = −0.0626 V) gives ΔEp = 0.1123 V or 112.3 mV, which is greater than 59/n mV. This is characteristic of a quasi-reversible electrochemical process. This result is confirmed by the ratio of the anodic peak current (Ipa = 4.91×10^{-5} A) to the cathodic peak current (|Ipc| = 1.13×10^{-4} A) is less than 1.

The plot of the redox peak currents (1 and 1') as a function of concentration (Figure 5B) shows linear relationships over the entire concentration range (0.1 - 0.6 mM), with determination coefficients ($R^2 = 0.993$ and $R^2 = 0.9985$) close to 1. This linearity confirms that the oxidation and reduction peak currents are proportional to the MB concentration. Therefore, the calibration equations obtained (Equations 9 and 10) indicate that this relationship can be used for the quantification of MB using the BDD electrode.

$$\mathrm{Ipa} = 0.0001[\mathrm{BM}] + 2\times10^{-06}, R^2 = 0.993 \quad (9)$$

$$\mathrm{Ipc} = -0.0002[\mathrm{BM}] + 1\times10^{-06}, R^2 = 0.999 \quad (10)$$

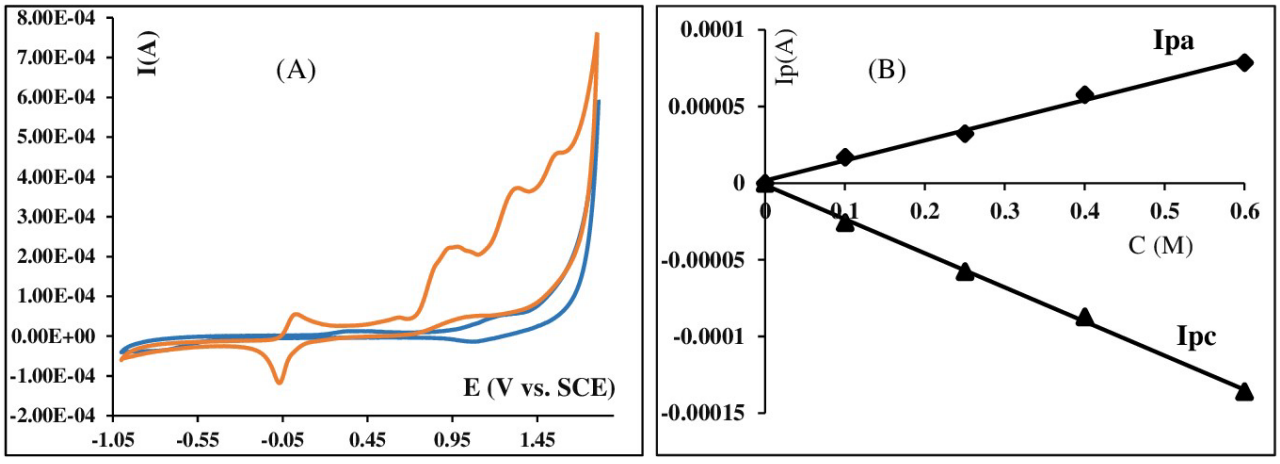

(A) (B)

Figure 5. (A) Cyclic voltammograms of the BDD electrode in sulfuric acid medium in the presence (red curve) and absence (blue curve) of MB at a scan rate of 50 mV/s, T = 25˚C. WE: BDD, CE: Pt wire, RE: SCE; (B) Representation of the peak current (anodic and cathodic) as a function of the concentration of the organic compound.

The effect of scan rate on the oxidation of MB (0.6 mM) was studied in a 0.1 M sulfuric acid electrolyte solution over a scan rate range of 20 to 200 mV/s, within a potential window from −1 to 1.8 V vs. SCE. The obtained voltammograms were used to determine the peak potentials and peak currents (for peaks 1 and 1'). **Figure 6(A)** shows the plot of Ip as a function of $v^{1/2}$. This representation allows for the analysis of the electrochemical reaction kinetics, identifying whether the process is controlled by diffusion and/or adsorption.

Indeed, if the relationship $Ip = f(v^{1/2})$ is linear and passes through the origin, the process at the electrode surface is governed by the diffusion of electroactive species to the electrode surface. Conversely, any deviation from linearity or significant intercept away from the origin would likely indicate an adsorption-controlled or mixed-control process.

The curves $Ipa = f(v^{1/2})$ and $Ipc = f(v^{1/2})$ for peaks 1 and 1' yield straight lines that nearly intersect the origin (Equations 11 and 12). This observation means that the oxidation and reduction processes at the electrode surface are diffusion-controlled.

$$Ipa = 0.0002v^{1/2} + 3\times10^{-06}, R^2 = 0.9889 \quad (11)$$

$$Ipc = -0.0003v^{1/2} - 7\times10^{-06}, R^2 = 0.9916 \quad (12)$$

The diffusion-controlled nature of the processes occurring at peaks 1 and 1' is confirmed by the plots of ln Ip vs. ln v (**Figure 6(B)**), which yield straight lines with slopes of 0.5002 and 0.4417 for the anodic and cathodic peaks, respectively (Equations 13 and 14). In fact, a slope close to 0.5 indicates a diffusion-controlled process, whereas a slope close to 1 suggests an adsorption-controlled process [28] [29].

$$\ln Ipa = 0.5002 \ln v - 8.593, R^2 = 0.9884 \quad (13)$$

$$\ln Ipc = 0.4417 \ln v - 8.1009, R^2 = 0.9914 \quad (14)$$

The speed of the electrochemical system was evaluated by analyzing the relationship between the potential and the logarithm of the scan rate. **Figure 6(C)** shows the resulting plots, which are straight lines with non-zero slopes (Equations 15 and 16) and determination coefficients close to 1, suggesting a slow electrochemical process characteristic of a non-reversible system.

$$Epa = 0.0185 \ln v + 0.0694, R^2 = 0.9998 \quad (15)$$

$$Epc = -0.0071 \ln v - 0.0808, R^2 = 0.9712 \quad (16)$$

3.3. Study of MB Oxidation in Sodium Sulfate (Na_2SO_4) Medium

Figure 7 presents the cyclic voltammograms of the BDD electrode in 0.1 M Na_2SO_4 medium, in the absence and presence of the organic compound, at 50 mV/s. In the cyclic voltammogram recorded in the absence of MB (inset of **Figure 7**), an anodic wave is observed between 1.33 and 1.80 V. The same observation was made in the H_2SO_4 medium. Additionally, the onset potentials for hydrogen and oxygen evolution are approximately −1.33 V and 1.80 V, respectively.

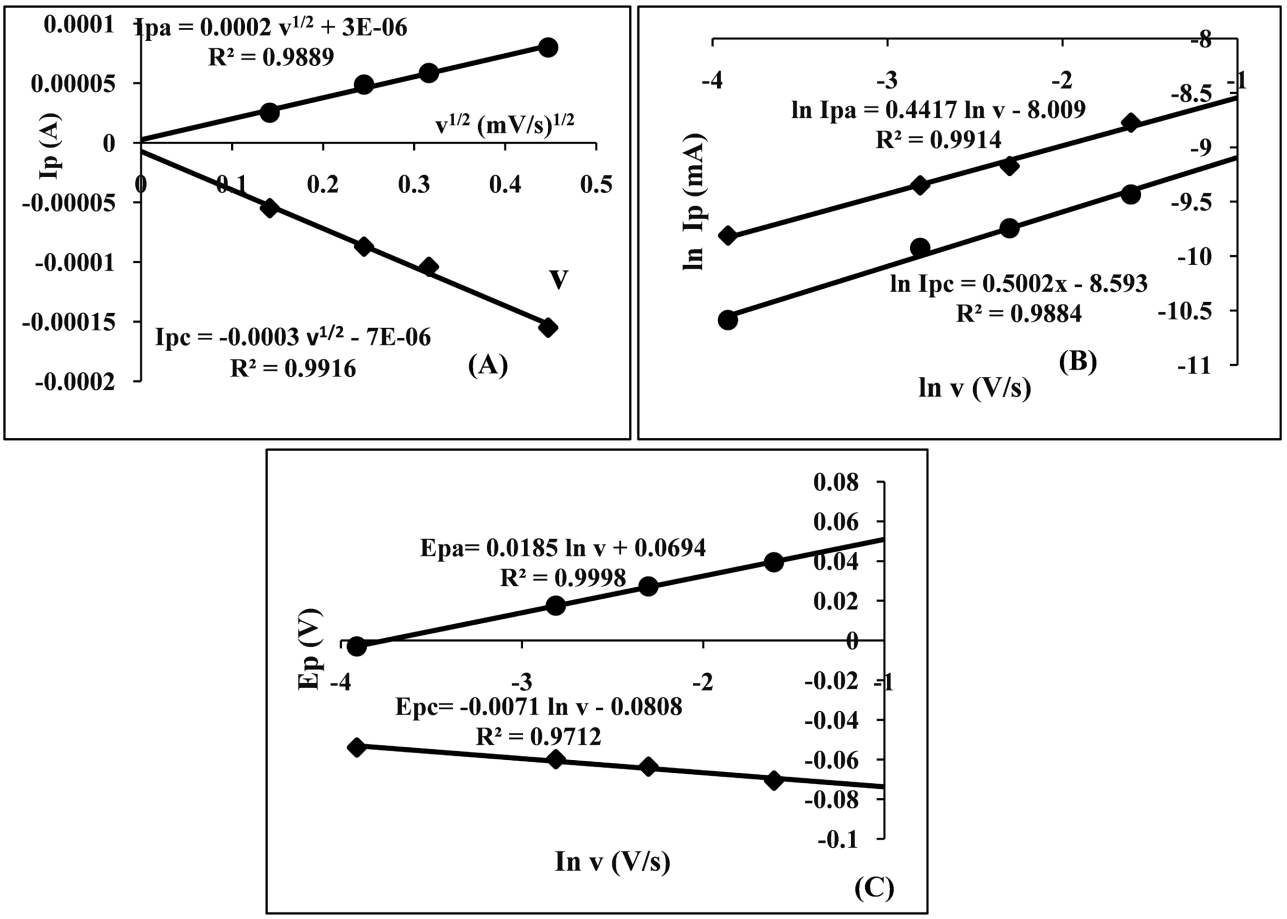

Figure 6. Cyclic voltammograms of the BDD electrode at 0.6 mM MB with various scan rates, from −1 to 1.8 V vs. SCE in sulfuric acid medium, T = 25˚C. WE: BDD, CE: Pt wire, RE: SCE. A) Plots of peak current vs. square root of scan rate; B) Plots of the logarithm of peak current vs. logarithm of scan rate; C) Plots of peak potential vs. logarithm of scan rate.

The voltammetric profile of the electrolyte solution containing MB (0.4 mM) exhibits the same general characteristics as those obtained in the sulfuric acid medium. The oxidation of MB in this medium is indicated by peaks, with four anodic peaks located at −0.33 V, 0.79 V, 1.2 V, and 1.43 V, and a cathodic peak at −0.44 V. All anodic peaks appear before the oxygen evolution potential (1.80 V), indicating a direct electron transfer oxidation process at the BDD surface. However, Peak 4 appears in the potential region corresponding to the anodic wave of the BDD in Na_2SO_4 alone, suggesting the involvement of oxidative sulfate species in the oxidation process observed at Peak 4. The MB oxidation could also be catalyzed the non-diamond carbon impurities such as Csp2 presents at the BDD's grain boundaries.

Moreover, in the presence of MB, a decrease in the oxygen evolution current at high potentials is observed, which suggests the involvement of oxidative species generated from water decomposition in the oxidation of MB.

According to the values obtained from the voltammogram in the presence of the organic compound (Figure 7), the difference between the anodic and cathodic peak potentials is greater than 59/n mV, and the Ipa/Ipc ratio is less than 1, char-

acteristics of a quasi-reversible electrochemical process.

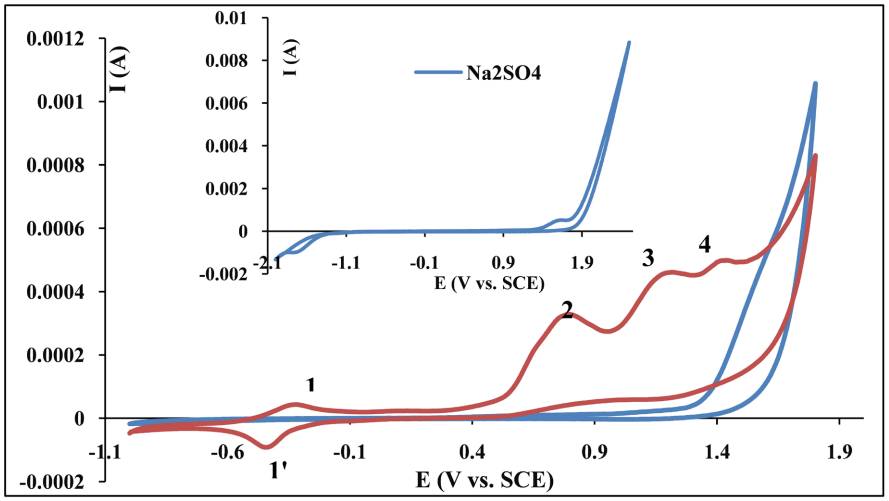

Figure 7. Cyclic voltammogram of the BDD electrode in sodium sulfate medium in the presence (red curve) and absence (blue curve) of MB at a scan rate of 50 mV/s, T = 25˚C. WE: BDD, CE: Pt wire, RE: SCE.

The plots of the redox peak currents (1 and 1') as a function of concentration (**Figure 8**) shows linear relationships over the entire concentration range from 0.1 to 0.4 mM for peak 1, and from 0.1 to 0.6 mM for peak 1'. The determination coefficients are close to 1, indicating excellent correlation between peak intensity and MB concentration (Equations 17 and 18). This linearity confirms that the oxidation and reduction peak currents are proportional to the MB concentration. However, in the case of anodic peak 1, it is observed that the current no longer increases when the methylene blue concentration exceeds 0.4 mM. Similar observations were reported by Ju *et al* in a supporting medium with a pH of 7.2 [30].

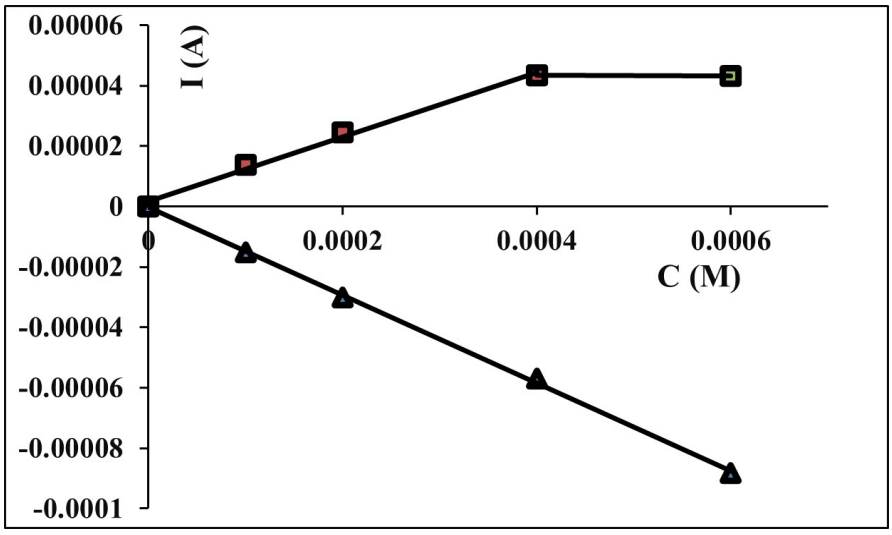

Figure 8. Plot of peak current variation as a function of methylene blue concentration. Scan rate = 50 mV/s, T = 25˚C. WE: BDD, CE: Pt wire, RE: SCE.

According to them, this phenomenon could be explained by the formation of dimers or larger aggregates at higher concentrations.

$$\text{Ipa} = 0.1066[\text{BM}] + 2\times10^{-06}, R^2 = 0.9923 \quad (17)$$

$$\text{Ipc} = -0.1455[\text{BM}] - 3\times10^{-07}, R^2 = 0.9992 \quad (18)$$

The effect of scan rate on the oxidation of MB (0.6 mM) was also studied in a 0.1 M Na_2SO_4 electrolyte solution over a scan rate range of 10 to 200 mV/s within a potential window from −1 to 1.8 V vs. SCE. The obtained voltammograms were used to determine the peak potentials and peak currents for peaks 1 and 1'. Figure 9(A) shows the plots of Ipa = f($v^{1/2}$) and Ipc = f($v^{1/2}$) for peaks 1 and 1' over the scan rate range of 10 to 200 mV/s. The resulting curves are linear with determination coefficients close to 1 (Equations 19 and 20). This observation indicates that the oxidation and reduction processes at the electrode surface are diffusion-controlled [31] [32].

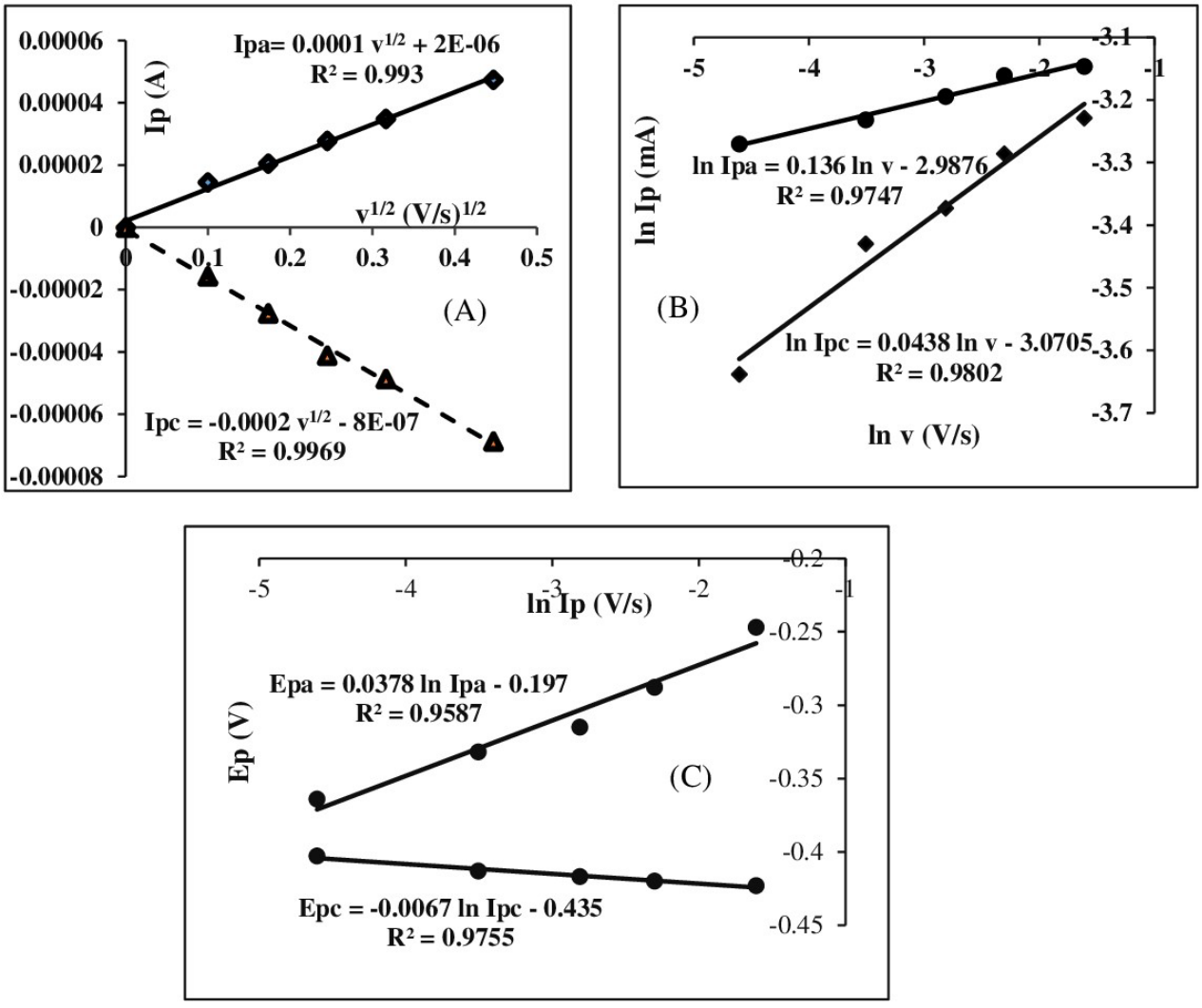

Figure 9. Plots of Ip versus $v^{1/2}$ (A), Ep versus log(v) (B), and the logarithm of anodic peak current versus the logarithm of scan rate (C).

$$Ipa = 0.0001v^{1/2} + 2\times10^{-06}, R^2 = 0.993 \quad (19)$$

$$Ipc = -0.0002v^{1/2} - 8\times10^{-07}, R^2 = 0.9961 \quad (20)$$

This result is consistent with that obtained from the plots of ln Ip versus ln v for the anodic and cathodic peaks [33] [34], where all slopes are less than 0.5 (**Figure 9(B)**).

The plot of Ep as a function of ln (v) is a straight line with a non-zero slope described by Equations 21 and 22 (**Figure 9(C)**):

$$Epa = 0.0378\ln Ipa - 0.197, R^2 = 0.9587 \quad (21)$$

$$Epc = -0.0067\ln Ipc - 0.435, R^2 = 0.9971 \quad (22)$$

This result suggests that the reaction is not fast. Moreover, the plot of $Ip = f(v^{1/2})$ is a straight line, which is characteristic of a quasi-reversible reaction.

3.4. Voltammetric Study of MB Oxidation in 0.1 M NaOH

The electrochemical behavior of MB (0.6 mM) on boron-doped diamond was studied within a potential range from −1 to 1.8 V in 0.1 M NaOH at a scan rate of 50 mV/s (**Figure 10**). The inset of **Figure 10** shows the cyclic voltammograms of the BDD electrode in the absence and presence of MB. In the absence of the compound, the cyclic voltammogram exhibits an anodic large peak located around at 1.44 V and an oxygen evolution potential started at 1.60 V. The anodic peak can be attributed to oxygen production through the oxidation of hydroxide, according to the redox couple O_2/OH^- (Equation 23).

$$OH^- \rightarrow 1/2\,O_2 + H^+ + 2e^- \quad (23)$$

In the forward potential scan, and the presence of MB in the reaction medium, an anodic wave appears starting at 0.33 V, indicating the oxidation of the organic compound. This oxidation occurs before the onset of oxygen evolution, suggesting that a direct oxidation process occurs at the surface of the BDD electrode. The

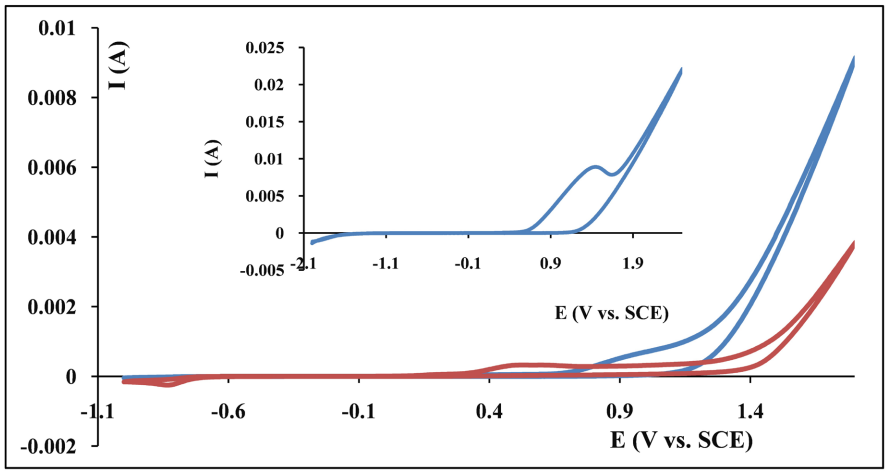

Figure 10. Cyclic voltammogram of the BDD electrode in sodium hydroxide medium in the presence (red curve) and absence (blue curve) of MB at a scan rate of 50 mV/s, T = 25˚C. WE: BDD, CE: Pt wire, RE: SCE.

lower current observed in the presence of MB compared to that obtained in the supporting electrolyte alone, in the high potential region, is characteristic of a mediated oxidation process involving oxidative species generated from the electrochemical discharge of water.

Unlike in H_2SO_4 and Na_2SO_4 media, the oxidation of MB in the basic NaOH (0.1 M) medium is characterized by a single anodic wave. This difference in electrochemical behavior can be attributed to the nature of the supporting electrolyte. In sulfuric acid and sodium sulfate supporting electrolytes, the oxidative species formed, notably the sulfate radical ($SO_4^{\bullet-}$) and the persulfate ion ($S_2O_8^{2-}$), exhibit higher selectivity toward electron-rich organic compounds, such as aromatic molecules and sulphur and nitrogen containing molecules. The oxidative species derived from sulfates react selectively with MB ($C_{16}H_{18}ClN_3S$) due to the presence of an aromatic ring and sulfur and nitrogen atoms in its structure [35]. This interaction leads to a multi-step oxidation mechanism based on direct electron transfers, without the involvement of strong oxidants before the onset of water oxidation.

Figure 11 illustrates the plot of current as a function of concentration at a fixed potential of 0.5 V. The MB concentration ranged from 0.1 to 0.4 mM, and voltammetric measurements were carried out at 50 mV/s. The resulting plot is a straight line described by the equation (Equation 24):

$$Ip = 0.0005[MB] + 6\times10^{-5}, R^2 = 0.9931 \quad (24)$$

The determination coefficient (R^2), close to 1, indicates excellent linearity of the relationship. This confirms that the BDD electrode can be used in NaOH medium for the quantification of MB.

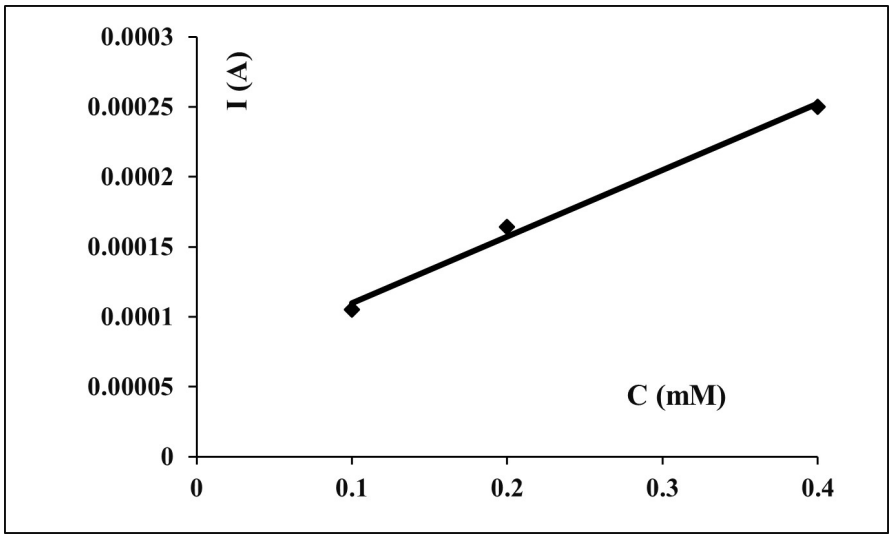

Figure 11. Plot of current intensity as a function of methylene blue concentration for potential fixed at 0.5 V vs SCE. Scan rate = 50 mV/s, T = 25˚C. WE: BDD, CE: Platinum wire, RE: SCE.

In this study, the effect of scan rate was investigated over a potential scan range

from 30 to 500 mV/s. The resulting cyclic voltammograms are shown in Figure 12. It can be observed that the oxidation wave of methylene blue increases with the scan rate.

To determine the oxidation process at the electrode, Ip versus the square root of scan rate was plotted at a fixed potential of 0.5 V.

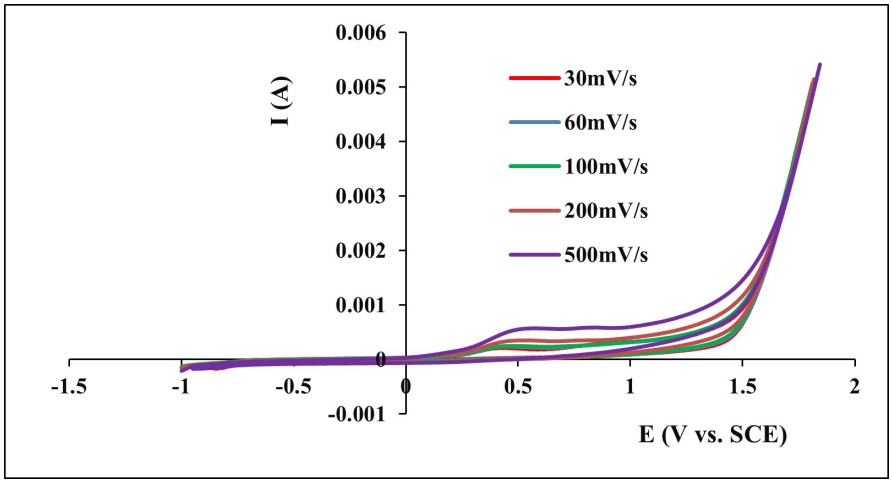

Figure 12. Cyclic voltammogram of the BDD electrode in 0.1 M NaOH containing 0.6 mM MB at different scan rates, T = 25˚C. WE: BDD, CE: rolled platinum wire, RE: SCE.

The plot of current versus the square root of the scan rate yields a straight line that does not pass through the origin, indicating that the oxidation of MB is diffusion-controlled, likely coupled with a chemical reaction or adsorption (Figure 13(A)).

In contrast, the plot of ln Ip = f(ln v), shown in Figure 13(B) (Equation 25), gives a straight line with a slope of 0.5567, close to 0.5, which is characteristic of a diffusion-controlled process.

$$\ln \mathrm{Ip}(\mathrm{A}) = 0.5567 \ln \mathrm{v} - 7.0653, \mathrm{R}^2 = 0.9957 \quad (25)$$

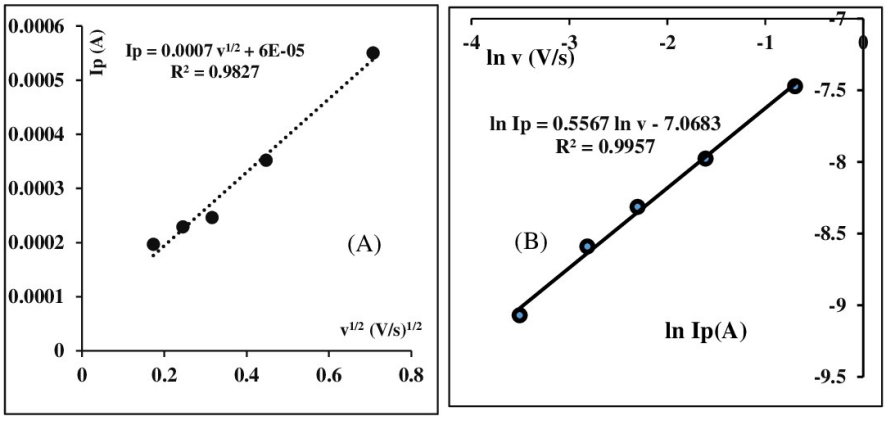

Figure 13. Evolution of the oxidation current intensity of MB as a function of the square root of the scan rate (A) and the natural logarithm of the scan rate (B) in 0.1 M NaOH, T = 25˚C. WE: BDD; CE: Platinum wire; RE: SCE.

3.5. Influence of Successive Cycles on Electrode Reactivity in the Presence of Methylene Blue

Previous studies have highlighted a polymerization phenomenon occurring at the surface of the working electrode during the electrochemical oxidation of certain organic compounds [14]. The formation of this polymeric film can hinder the oxidation reaction or alter the electrochemical behavior of the electrode. In the present study, the influence of the number of scan cycles on the shape of the voltammograms in the presence of methylene blue (MB) was investigated in different supporting electrolytes. The results obtained in Na_2SO_4 and NaOH media are presented in **Figure 14**, for a fixed scan rate of 50 mV/s. In both media, a gradual decrease in the anodic current is observed from the first cycles, until a superposition of the curves is reached, an indication of a stable electrochemical behaviour, starting from the 5th cycle in NaOH and the 12th cycle in Na_2SO_4. These observations suggest that the oxidation of MB on BDD leads to the formation of a polymeric film on the electrode surface. Moreover, the stabilization of the anodic current may result from the low adsorption capacity of BDD, which is related to the inert nature of its surface. A similar behavior was also observed in H_2SO_4 medium (figure not shown), where the current decreases up to the 4th cycle, followed by a superposition of the voltammetric curves in the anodic domain.

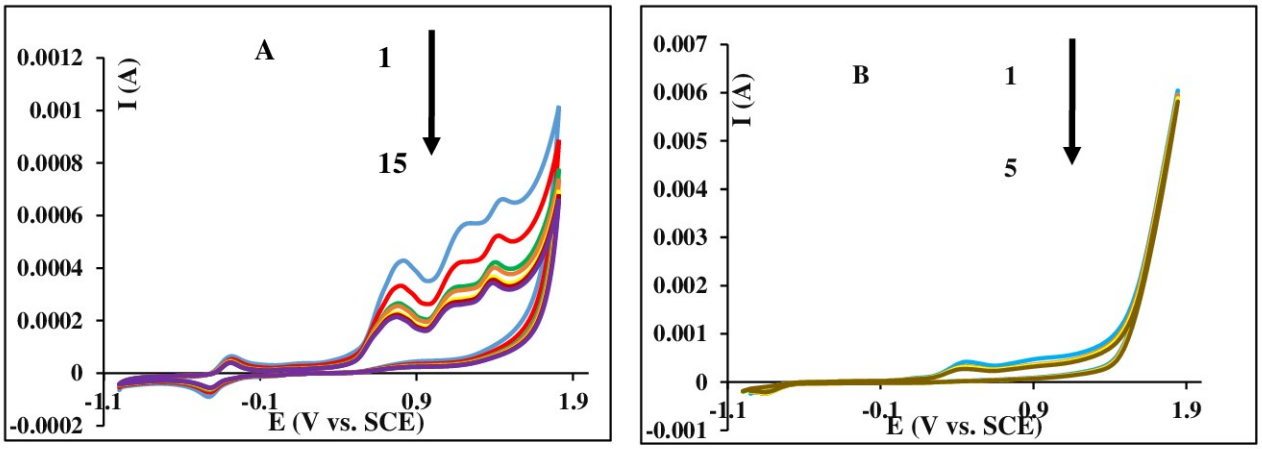

Figure 14. Cyclic voltammetry curves recorded on boron-doped diamond electrodes over several successive scans in 0.6 mM methylene blue solution containing 0.1 M sodium sulfate (A) and 0.1 M sodium hydroxide (B). Scan rate= 50 mV/s, WE: BDD, CE: Pt wire, T = 25°C, RE: SCE.

4. Conclusions

Based on the present study, the boron-doped diamond (BDD) electrode exhibits a polycrystalline structure, with surface grains ranging from 0.3 to 0.6 µm. In addition to diamond (Csp3) crystal, the BDD surface also contains non-diamond carbon impurities (Csp_2) *i.e.*, graphitic-type carbon.

Electrochemical analysis in various supporting electrolytes revealed the appearance of anodic waves in both H_2SO_4 and Na_2SO_4 media, within potential windows of 1.40 - 1.85 V and 1.33 - 1.80 V, close to the onset of oxygen evolution, respec-

tively. These features suggest the likely formation of sulphate derived oxidative species and/or the oxidation of the Csp2 present at the BDD's grain boundaries. In the NaOH medium, the electrochemical response showed a distinct anodic peak attributed to oxygen evolution.

The oxidation of methylene blue (MB) was characterized by four anodic peaks in H_2SO_4 and Na_2SO_4, and by a broad anodic wave in NaOH. In H_2SO_4, anodic peaks were observed at 0.035 V, 0.94 V, 1.34 V, and 1.57 V, while the cathodic peak appeared at approximately –0.063 V. In Na_2SO_4, the anodic peaks occurred at –0.33 V, 0.79 V, 1.2 V, and 1.47 V, with the corresponding cathodic peak located around –0.44 V. In NaOH, a broad anodic wave began at 0.33 V.

These results indicate that MB oxidation in the different media may proceed via both direct electron transfer at the electrode surface and indirect oxidation mediated by reactive oxidative species. The electrochemical process is quasi-reversible, as evidenced by the peak potential separation (ΔEp) exceeding 59 mV and by Ipa/Ipc ratios deviating from unity. Furthermore, the oxidation process is diffusion-controlled. Notably, successive cyclic voltammetry scans revealed the formation of a polymeric film on the electrode surface.

Conflicts of Interest

The authors declare no conflicts of interest regarding the publication of this paper.

References

[1] Alegbe, E.O. and Uthman, T.O. (2024) A Review of History, Properties, Classification, Applications and Challenges of Natural and Synthetic Dyes. *Heliyon*, **10**, e33646. https://doi.org/10.1016/j.heliyon.2024.e33646

[2] Pizzicato, B., Pacifico, S., Cayuela, D., Mijas, G. and Riba-Moliner, M. (2023) Advancements in Sustainable Natural Dyes for Textile Applications: A Review. *Molecules*, **28**, Article 5954. https://doi.org/10.3390/molecules28165954

[3] Kapanga, P.M., Nyakairu, G.W.A., Nkanga, C.I., Lusamba, S.N., Tshimanga, R.M. and Shehu, Z. (2024) A Review of Dye Effluents Polluting African Surface Water: Sources, Impacts, Physicochemical Properties, and Treatment Methods. *Discover Water*, **4**, Article No. 85. https://doi.org/10.1007/s43832-024-00129-2

[4] Dutta, S., Adhikary, S., Bhattacharya, S., Roy, D., Chatterjee, S., Chakraborty, A., *et al.* (2024) Contamination of Textile Dyes in Aquatic Environment: Adverse Impacts on Aquatic Ecosystem and Human Health, and Its Management Using Bioremediation. *Journal of Environmental Management*, **353**, Article ID: 120103. https://doi.org/10.1016/j.jenvman.2024.120103

[5] Lin, J., Ye, W., Xie, M., Seo, D.H., Luo, J., Wan, Y., *et al.* (2023) Environmental Impacts and Remediation of Dye-Containing Wastewater. *Nature Reviews Earth & Environment*, **4**, 785-803. https://doi.org/10.1038/s43017-023-00489-8

[6] Oladoye, P.O., Ajiboye, T.O., Omotola, E.O. and Oyewola, O.J. (2022) Methylene Blue Dye: Toxicity and Potential Elimination Technology from Wastewater. *Results in Engineering*, **16**, Article ID: 100678. https://doi.org/10.1016/j.rineng.2022.100678

[7] Bužga, M., Machytka, E., Dvořáčková, E., Švagera, Z., Stejskal, D., Máca, J., *et al.*

(2022) Methylene Blue: A Controversial Diagnostic Acid and Medication? *Toxicology Research*, **11**, 711-717. https://doi.org/10.1093/toxres/tfac050

[8] Lipskikh, O.I., Korotkova, E.I., Khristunova, Y.P., Barek, J. and Kratochvil, B. (2018) Sensors for Voltammetric Determination of Food Azo Dyes—A Critical Review. *Electrochimica Acta*, **260**, 974-985. https://doi.org/10.1016/j.electacta.2017.12.027

[9] Mazzeo, L., Marzi, D., Bavasso, I., Piemonte, V. and Di Palma, L. (2023) Removal of Methylene Blue from Wastewater by Waste Roots from the Arsenic-Hyperaccumulator Pteris Vittata: Fixed Bed Adsorption Kinetics. *Materials*, **16**, Article 1450. https://doi.org/10.3390/ma16041450

[10] Tubon-Usca, G., Centeno, C., Pomasqui, S., Beneduci, A. and Arias, F.A. (2025) Enhanced Adsorption of Methylene Blue in Wastewater Using Natural Zeolite Impregnated with Graphene Oxide. *Applied Sciences*, **15**, Article 2824. https://doi.org/10.3390/app15052824

[11] Appia, F.T.A., Kouassi, T.G.D., Kimou, K.J., Coulibaly, C.S., Meledje, J. and Ouattara, L. (2025) Photolytic Degradation of Methylene Blue: The Effect of Various Factors on Wastewater Treatment Efficiency. *Asian Journal of Chemical Sciences*, **15**, 41-52. https://doi.org/10.9734/ajocs/2025/v15i1347

[12] Abdrabou, D., Ahmed, M., Hussein, A. and El-Sherbini, T. (2023) Photocatalytic Behavior for Removal of Methylene Blue from Aqueous Solutions via Nanocomposites Based on Gd_2O_3/CdS and Cellulose Acetate Nanofibers. *Environmental Science and Pollution Research*, **30**, 99789-99808. https://doi.org/10.1007/s11356-023-28999-4

[13] Loba, E.M.H., Appia, F.T.A., Kouassi, T.G.D., Koné, S., Yao, K.F. and Kouassi, K.K.E. (2023) Anodic Oxidation of Cationic Dye on Boron-Doped Diamond (BDD): Effect of Electrochemical Operation Parameters. *RAMReS Sciences des Structures et de la Matière*, **7**, 20-36.

[14] Gnamba, C.Q., Appia, F.T.A., Loba, E.M.H., Sanogo, I. and Ouattara, L. (2015) Electrochemical Oxidation of Amoxicillin in Its Pharmaceutical Formulation at Boron Doped Diamond (BDD) Electrode. *Journal of Electrochemical Science and Engineering*, **5**, 129-143. https://doi.org/10.5599/jese.186

[15] Pop, A., Manea, F., Flueras, A. and Schoonman, J. (2017) Simultaneous Voltammetric Detection of Carbaryl and Paraquat Pesticides on Graphene-Modified Boron-Doped Diamond Electrode. *Sensors*, **17**, Article 2033. https://doi.org/10.3390/s17092033

[16] Gimadutdinova, L., Ziyatdinova, G. and Davletshin, R. (2023) Selective Voltammetric Sensor for the Simultaneous Quantification of Tartrazine and Brilliant Blue FCF. *Sensors*, **23**, Article 1094. https://doi.org/10.3390/s23031094

[17] Sun, J., Lu, H., Du, L., Lin, H. and Li, H. (2011) Anodic Oxidation of Anthraquinone Dye Alizarin Red S at Ti/BDD Electrodes. *Applied Surface Science*, **257**, 6667-6671. https://doi.org/10.1016/j.apsusc.2011.02.099

[18] Tang, Y., He, D., Guo, Y., Qu, W., Shang, J., Zhou, L., *et al.* (2020) Electrochemical Oxidative Degradation of X-6G Dye by Boron-Doped Diamond Anodes: Effect of Operating Parameters. *Chemosphere*, **258**, Article ID: 127368. https://doi.org/10.1016/j.chemosphere.2020.127368

[19] Lee, T., You, M., Kim, S. and Song, P. (2025) The Growth Mechanism of Boron-Doped Diamond in Relation to the Carbon-to-Hydrogen Ratio Using the Hot-Filament Chemical Vapor Deposition Method. *Micromachines*, **16**, Article 742. https://doi.org/10.3390/mi16070742

[20] Li, Z., Zhou, B., Yang, W., Deng, Z., Chen, F., Bai, H., *et al.* (2023) The Effect of Boron Doping Concentration on the Electrochemical Oxidation of Chlorine Using BDD Electrode. *Journal of The Electrochemical Society*, **170**, Article ID: 033502.

https://doi.org/10.1149/1945-7111/acad2d

[21] Long, H., Hu, H., Wen, K., Liu, X., Liu, S., Zhang, Q., *et al.* (2023) Thickness Effects on Boron Doping and Electrochemical Properties of Boron-Doped Diamond Film. *Molecules*, **28**, Article 2829. https://doi.org/10.3390/molecules28062829

[22] Adar, F. (2022) Use of Raman Spectroscopy to Qualify Carbon Materials. *Spectroscopy*, **37**, 11-15, 50. https://doi.org/10.56530/spectroscopy.wx3481u2

[23] Chen, L., Lei, C., Li, Z., Yang, B., Zhang, X. and Lei, L. (2018) Electrochemical Activation of Sulfate by BDD Anode in Basic Medium for Efficient Removal of Organic Pollutants. *Chemosphere*, **210**, 516-523. https://doi.org/10.1016/j.chemosphere.2018.07.043

[24] Zhang, F., Sun, Z. and Cui, J. (2020) Research on the Mechanism and Reaction Conditions of Electrochemical Preparation of Persulfate in a Split-Cell Reactor Using BDD Anode. *RSC Advances*, **10**, 33928-33936. https://doi.org/10.1039/d0ra04669h

[25] Serrano, K., Michaud, P.A., Comninellis, C. and Savall, A. (2002) Electrochemical Preparation of Peroxodisulfuric Acid Using Boron Doped Diamond Thin Film Electrodes. *Electrochimica Acta*, **48**, 431-436. https://doi.org/10.1016/s0013-4686(02)00688-6

[26] Svitková, V. and Vyskočil, V. (2022) Electrochemical Behavior of Methylene Blue at Bare and DNA-Modified Silver Solid Amalgam Electrodes. *Journal of Solid State Electrochemistry*, **26**, 2491-2499. https://doi.org/10.1007/s10008-022-05270-3

[27] Liu, B., Cang, H., Cui, L. and Zhang, H. (2017) Electrochemical Polymerization of Methylene Blue on Glassy Carbon Electrode. *International Journal of Electrochemical Science*, **12**, 9907-9913. https://doi.org/10.20964/2017.10.49

[28] Porat, Z. (2024) Electrochemical Characterization of Diffusion in Polymeric Vs. Monomeric Solvents. *International Journal of Molecular Sciences*, **25**, Article 4472. https://doi.org/10.3390/ijms25084472

[29] Nguyen, H. (2022) Insight into Electrochemical Degradation of Cartap (in Padan 95SP) by Boron-Doped Diamond Electrode: Kinetic and Effect of Water Matrices. *Turkish Journal of Chemistry*, **46**, 1733-1743. https://doi.org/10.55730/1300-0527.3476

[30] Ju, H., Zhou, J., Cai, C. and Chen, H. (1995) The Electrochemical Behavior of Methylene Blue at a Microcylinder Carbon Fiber Electrode. *Electroanalysis*, **7**, 1165-1170. https://doi.org/10.1002/elan.1140071213

[31] He, S., Lin, K., Cheng, S., Gao, N., Liu, J. and Li, H. (2024) Improving Trace Detection of Methylene Blue by Designing Nanowire Array on Boron-Doped Diamond as Electrochemical Electrode. *Coatings*, **14**, Article 762. https://doi.org/10.3390/coatings14060762

[32] Masood, Z., Muhammad, H. and Tahiri, I.A. (2024) Comparison of Different Electrochemical Methodologies for Electrode Reactions: A Case Study of Paracetamol. *Electrochem*, **5**, 57-69. https://doi.org/10.3390/electrochem5010004

[33] Nabatian, E., Mousavi, M., Pournamdari, M., Yoosefian, M. and Ahmadzadeh, S. (2022) Voltammetric Approach for Pharmaceutical Samples Analysis; Simultaneous Quantitative Determination of Resorcinol and Hydroquinone. *BMC Chemistry*, **16**, Article No. 115. https://doi.org/10.1186/s13065-022-00905-y

[34] Koffi, K.S., Appia, F.T.A., Kouadio; K.E., Kimou, K.J., Souleymane, K. and Lassiné, O. (2021) Cyclic and Differential Pulse Voltammetry Investigations of an Diiodine Contrast Product Using Microelectrode of BDD. *Mediterranean Journal of Chemistry*, **11**, 244-254.

[35] Feijoo, S., Baluchová, S., Kamali, M., Buijnsters, J.G. and Dewil, R. (2024) A Combined Experimental and Computational Approach to Unravel Degradation Mechanisms in Electrochemical Wastewater Treatment. *Environmental Science*: *Water Research & Technology*, **10**, 652-667. https://doi.org/10.1039/d3ew00784g